Analysis of Numerical Errors in Solving Particle Langevin Equations

by

J. Xu and S.B. Pope

FDA 97-07 June 1997

1 Introduction

In PDF methods for modeling turbulent reactive flows, the fluid within the solution domain is usually represented by a large number of computational particles whose properties, e.g. velocities, evolve according to modeled stochastic differential equations based on turbulence theory [6]. These stochastic differential equations are essentially Langevin equations. A particle–mesh method is then adopted to solve the Langevin equations, which is equivalent to solving the PDF transport equations [7]. The basic techniques involved in the numerical schemes are time marching and finite difference [5]. Accordingly, several supplementary numerical techniques, such as variance reduction and time averaging, have been introduced for improving the solution [7]. Some of the numerical issues pertinent to PDF methods have been investigated in several studies [2][10][12]. This report, however, analyzes theoretically a simplified model of fluid particles to investigate certain numerical errors in PDF methods. Specifically, a theoretical analysis is presented of the numerical errors arising from the use of the ensemble mean (to approximate the mean) in the drift term in the Langevin equations. Previously [12], this approximation has been shown empirically to lead to significant bias. The following section describes the model problem. The models are then solved in section 3. The results are discussed in the final section.

2 Model Problem

In the context of PDF methods for turbulent flows, the flow is regarded as a stochastic field. The motion of fluid particles is then modeled by the stochastic differential equations: Langevin equations. For any particle property x, the evolution equation usually has the form [6] [7],

$$dx = -\frac{(x - \langle x \rangle)}{T} dt + b dW, \tag{1}$$

where $\langle x \rangle$ is the mean or expectation of x, T is a time scale, b is a positive constant and W is a Wiener process:

$$\langle dW dW \rangle = dt. \tag{2}$$

The detailed form and the variables of Eq.(1) for turbulence models are discussed in [6] [8]. Furthermore, the particle equation Eq.(1) is then solved numerically by a particle–mesh method [7]. In this study, both the physical model and the numerical algorithms involved in PDF methods are simplified and analyzed to investigate the numerical errors in PDF methods.

2.1 Physical Model

A simplified model of Eq.(1) is described here. Supposing the fluid is represented by N particles, the evolution of the property x_i of the ith particle (for $i = 1, \ldots, N$) is modeled by the following equation

$$dx_i = -(x_i - \alpha\langle x\rangle)dt + \sqrt{2}dW_i, \tag{3}$$

$$x_i(t=0) = c_i, \tag{4}$$

where $\langle x_i\rangle = \langle x\rangle$, $\langle dW_i dW_j\rangle = \delta_{ij}dt$, α is a constant and the time-scale has been taken to be unit. The initial conditions c_i are taken to be independent standardized normally distributed random variables:

$$\langle c_i\rangle = 0, \qquad \langle c_i c_j\rangle = \delta_{ij}. \tag{5}$$

The linear stochastic equation Eq.(3) describes the particle behavior in a homogeneous field. The N particles thus form a linear system of stochastic differential equations. According to Arnold [1], $\langle x\rangle$ is the solution of the deterministic linear differential equation:

$$\frac{d\langle x\rangle}{dt} = -(\langle x\rangle - \alpha\langle x\rangle), \tag{6}$$

$$\langle x(t=0)\rangle = \langle c_i\rangle = 0. \tag{7}$$

The solution for $\langle x\rangle$ is trivial. However, if the initial condition is not zero for $\langle x\rangle$, then it can been seen that for $\alpha < 1$, Eq.(3) is stable and eventually reaches the stationary state with $\langle x_i\rangle = 0$ and $var(x_i) = 1$ or $\langle x_i x_i\rangle = 1$. For $\alpha > 1$, the equation becomes unstable with $\langle x\rangle$ growing exponentially. For $\alpha = 1$, the equation is neutrally stable. How α determines the properties of Eq.(3) is discussed further below.

On the other hand, the covariance of the components x_i and x_j is defined as

$$Cov(x_i, x_j) = \langle (x_i - \langle x\rangle)(x_j - \langle x\rangle)\rangle \tag{8}$$

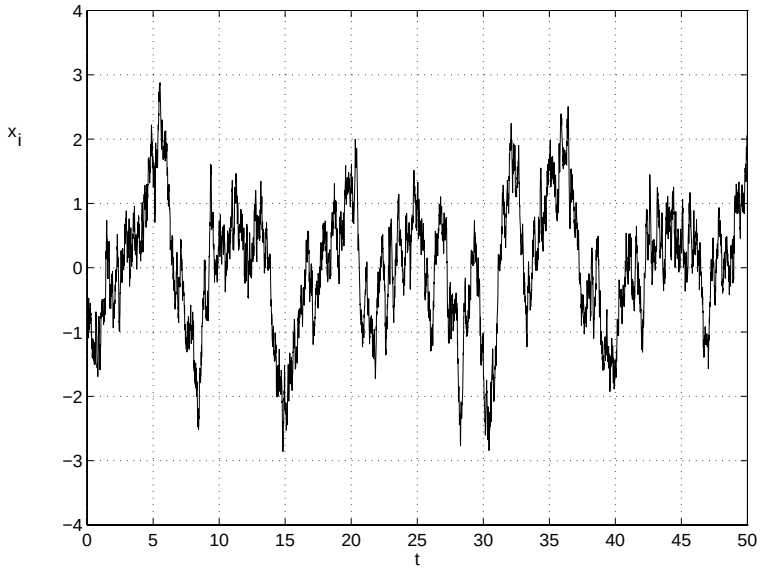

Figure 1: The typical trajectory of property x_i.

The solution for $Cov(x_i, x_j)$ when $\langle x \rangle = 0$ is

$$Cov(x_i, x_j) = \delta_{ij}. \tag{9}$$

It shows that the properties of particles have independent and identical distribution with zero mean and unit variance.

To summarize, there exists a stationary solution for Eq.(3)

$$\langle x_i \rangle = 0, \qquad var(x_i) = 1, \qquad \text{for} \;\; i = 1, \ldots, N. \tag{10}$$

Therefor, x_i is an Ornstein-Uhlenbeck process whose behavior is fully described by the mean and the covariance. A typical trajectory of x_i evolving by Eq.(3) is shown in Fig.(1).

2.2 Numerical Model

Several different approaches have been suggested for the numerical solution of stochastic differential equations such as Eq.(1) or Eq.(3) when $\langle x \rangle$ is determined. The various schemes of different orders and their accuracy are well studied [5]. However, it is noted that for solving Eq.(1) or Eq.(3) numerically, an estimate for $\langle x \rangle$ is needed. This is significant since

it introduces the new feature of the numerical errors in implementing the PDF methods [7][12]. As usual, the ensemble mean of all particles is used to approximate $\langle x \rangle$ [3]. That is

$$\langle x \rangle \simeq \{x\} \equiv \frac{1}{N} \sum_{i=1}^{N} x_i. \tag{11}$$

Consequently, Eq.(3) becomes

$$dx_i = -(x_i - \alpha\{x\})dt + \sqrt{2}dW_i. \tag{12}$$

or

$$dx_i = -(x_i - \frac{\alpha}{N} \sum_{i=1}^{N} x_i)dt + \sqrt{2}dW_i, \qquad \text{for } i = \ldots, N. \tag{13}$$

Hence the stochastic equations really solved in the PDF methods are Eq.(13) instead of the exact equations Eq.(3). The difference between the solutions of these equations is the numerical error which is discussed in this study. Equation (13) forms a system of N stochastic differential equations. It is the basic model of this study and its solution will be discussed in next section.

Moreover, in the numerical calculations using PDF methods, for stationary flows the time-averaging technique can be used to reduce the fluctuations in the estimate of the mean resulting from the finite number of particles or samples [9]. It is also expected that the numerical error of bias can be reduced by decreasing these fluctuations [12]. The time-averaging value y for $\{x\}$ is calculated by:

$$dy = -\Omega(y - \{x\})dt, \tag{14}$$

where Ω is the time-averaging scale [11]. Making use of y to estimate $\langle x \rangle$, the stochastic system Eq.(3) becomes

$$dx_i = -(x_i - \alpha y)dt + \sqrt{2}dW_i, \tag{15}$$

$$dy = -\Omega(y - \frac{1}{N} \sum_{i=1}^{n} x_i)dt, \qquad \text{for }, i = 1, \ldots, N \tag{16}$$

Equations (15) and (16) form a set of $N + 1$ coupled stochastic differential equations. Note that in the limit $\Omega \to \infty$, y tends to the ensemble mean $\{x\}$ and thus Eq.(15) becomes identical to Eq.(13).

Both the systems of Eq.(13) and Eqs.(15), (16) can be written in the vector form

$$d\mathbf{z} = \mathbf{A}\mathbf{z}dt + \mathbf{B}d\mathbf{W}, \tag{17}$$

where $\mathbf{z}$, $\mathbf{A}$ and $\mathbf{B}$ will be described in the following section, $d\mathbf{W}$ is the vector of the independent Wiener process. The initial conditions for Eq.(17) are defined as

$$\mathbf{z} = \mathbf{c} \qquad \text{at} \quad t = 0, \tag{18}$$

and $\mathbf{c}$ is a random vector having normal distribution (with mutually independent components) and satisfies

$$\langle \mathbf{c} \rangle = 0, \qquad \langle \mathbf{c}\mathbf{c}^T \rangle = \mathbf{K}, \tag{19}$$

where $\mathbf{K}$ is the covariance matrix for $\mathbf{z}$. Only for such an initial condition does Eq.(17) have a stationary solution [1]. The solution for $\mathbf{K}$ are discussed in the next section as well as the properties of Eq.(17).

In the process of seeking a numerical solution for the physical model Eq.(3), the equations one solves are indeed the equations of (13) or (15) and (16) because the real mean or expectation $\langle x \rangle$ is replaced by $\{x\}$ or y respectively. The numerical model should converge to the physical model as $N \to \infty$. The difference between the two models are thus defined as the numerical errors that are, especially the bias error, analyzed in this study. The bias is defined as the deterministic error due to the finite number of particles [7][12]. For example, the bias of the variance in the numerical model is

$$b_{var} \equiv var(x_i) - var(x_i)|_{N\to\infty}, \tag{20}$$

$$= var(x_i) - 1, \tag{21}$$

where the solution of physical model has been substituted in. Clearly, when the mean is approximated by the ensemble mean or the time-averaged value, a bias error will be introduced.

The properties of the numerical model is discussed in the next section as well as the solution for $\mathbf{K}$. The analysis presents a view about the bias in the PDF methods.

3 Analysis of Numerical Models

The numerical models defined in the forgoing section are solved as stochastic differential systems in this section. First of all, Eq.(13) and Eqs.(15), (16) are rewritten in the vector form

$$d\mathbf{z} = \mathbf{A}\mathbf{z}dt + \mathbf{B}d\mathbf{W}, \tag{22}$$

as mentioned in the previous section. In this section, an analysis is performed for the system with the time-averaging technique, i.e. Eq.(15) and Eq.(16) in detail, and the solution for Eq.(13) can in accordance be deduced from the solution of Eq.(15) and Eq.(16) for $\Omega \to \infty$.

Rewriting Eq.(15) and Eq.(16) in the form of Eq.(22), we have

$$\mathbf{z} = [x_1, x_2, \ldots, x_N, y]^T, \tag{23}$$

$$\mathbf{A} = \begin{bmatrix} -\mathbf{I} & \alpha\mathbf{w}^T \\ \frac{\Omega}{N}\mathbf{w} & -\Omega \end{bmatrix}_{(N+1)^2}, \tag{24}$$

$$\mathbf{B} = \sqrt{2}\begin{bmatrix} \mathbf{I} & 0 \\ 0 & 0 \end{bmatrix}_{(N+1)^2}, \tag{25}$$

where

$$\mathbf{w} = [1, 1, \ldots, 1]_N. \tag{26}$$

The initial conditions for Eq.(22) are assigned as

$$\mathbf{z} = \mathbf{c}, \qquad \text{at} \quad t = 0. \tag{27}$$

The properties of the random vector $\mathbf{c}$ is discussed below.

3.1 Stationarity

The physical model of Eq.(3) yields a stationary solution for the particle properties as shown in the previous section. Correspondingly, a stationary process should be sought for the numerical model as well. The linear stochastic differential equations Eqs.(22) has been well

studied. As pointed out by Arnold [1], The stochastic process is stationary if and only if

$$\begin{aligned} \langle \mathbf{z} \rangle &= const, \qquad (28) \\ \mathbf{K}(s,t) &\equiv \langle (\mathbf{z}(s) - \langle \mathbf{z}(s) \rangle)(\mathbf{z}(t) - \langle \mathbf{z}(t) \rangle) \rangle \\ &= \overline{\mathbf{K}}(s-t) \qquad (29) \end{aligned}$$

These conditions are satisfied if [1]

1. The matrices $\mathbf{A}$ and $\mathbf{B}$ are both independent of t
2. The initial conditions $\mathbf{c}$ is normally distributed with zero mean and the variance $\mathbf{K}$

$$\mathbf{K} = \overline{\mathbf{K}}(0) \qquad (30)$$

3. The eigenvalues of $\mathbf{A}$ are negative.

For the numerical model, we can see that the first condition is automatically satisfied. On the other hand, the requirements for the initial conditions are presumedly satisfied as well (Eq.(19)). Thus, the stationarity of the process fully depends on the coefficient matrix $\mathbf{A}$, i.e., $\mathbf{A}$ essentially determines the feature of the system.

Suppose that an eigenvalue of $\mathbf{A}$ is λ, then

$$| \lambda \mathbf{I} - \mathbf{A} | = 0. \qquad (31)$$

It follows that

$$| \lambda \mathbf{I} - \mathbf{A} | = \begin{vmatrix} \lambda+1 & & & & -\alpha \\ & \lambda+1 & & & -\alpha \\ & & \dots & & \vdots \\ & & & \lambda+1 & -\alpha \\ -\frac{\Omega}{N} & -\frac{\Omega}{N} & \dots & -\frac{\Omega}{N} & \lambda+\Omega \end{vmatrix}_{(N+1)^2} \qquad (32)$$

$$= (\lambda+1)^{N-1}[\lambda^2 + (\Omega+1)\lambda + \Omega(1-\alpha)] \qquad (33)$$

Then, the eigenvalues of $\mathbf{A}$ are readily solved as

$$\lambda_i = -1, \qquad \text{for } i = 1, 2, \ldots, N-1, \tag{34}$$

$$\lambda_N = \frac{-(\Omega+1) - \sqrt{(\Omega-1)^2 + 4\alpha\Omega}}{2} < 0, \tag{35}$$

$$\lambda_{N+1} = \frac{-(\Omega+1) + \sqrt{(\Omega-1)^2 + 4\alpha\Omega}}{2}. \tag{36}$$

It is clear that for $\alpha \geq 1$, λ_{N+1} is not negative, which therefore leads to an unstationary solution [1], whereas for $\alpha < 1$, all the eigenvalues are negative real numbers so that the stationary solution exists. Thus, to ensure the stationarity of Eq.(22), α is chosen less than 1.

For this study, all three conditions are then satisfied so that the numerical models are stationary Gaussian processes [1].

On the other hand, for general t, $s \geq 0$, one obtains

$$\mathbf{K}(s,t) = \overline{\mathbf{K}}(s-t) = \begin{cases} e^{\mathbf{A}(s-t)}\mathbf{K}, & s \geq t, \\ \mathbf{K}e^{\mathbf{A}^T(s-t)}, & s < t. \end{cases} \tag{37}$$

and the time scale matrix $\mathbf{T}$ is defined as

$$\mathbf{T} = \int_0^\infty \overline{\mathbf{K}}(\tau) d\tau. \tag{38}$$

It can be seen that the time scale is essentially determined by the eigenvalues of the matrix $\mathbf{A}$: the larger the absolute value of the eigenvalue is, the shorter the time scale is. In the presence of time-averaging technique, when the larger time scale (the smaller Ω) is chosen, the smaller the absolute value of eigenvalue of λ_{N+1} is (Fig.(2)), which in turn introduces a long time scale in the solution.

3.2 Analysis of Numerical Errors

Because the numerical model becomes a stationary Gaussian process, its properties are fully described by the mean and the covariance matrix. As for the mean $\langle x_i \rangle$, the numerical model with the initial conditions described above gives the same result as the physical model. The variance of $\langle x_i \rangle$ is, however, different between the physical model and the numerical model.

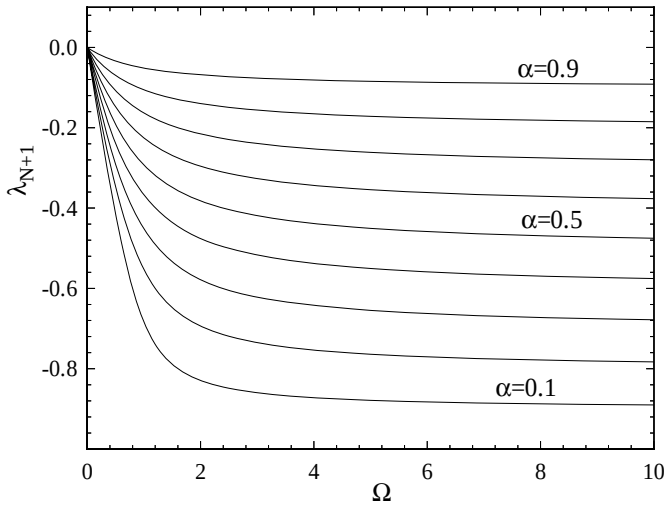

Figure 2: The eigenvalue λ_{N+1} against Ω for different α.

The solution for the variance are obtained and then compared to that of the physical model to investigate the bias of the variance. To solve for the variance, one basically needs to calculate the covariance matrix $\mathbf{K}$ for the numerical model.

According to Arnold [1], the solution of $\mathbf{K}$ to Eq.(22) is

$$\mathbf{K} = \int_0^\infty e^{\mathbf{A}t}\mathbf{B}\mathbf{B}^T e^{\mathbf{A}^T t} dt. \tag{39}$$

If the eigenvalues of $\mathbf{A}$ are negative (the case for $\alpha < 1$), Eq.(39) can be integrated by parts so that the above equation can be equivalently solved through [1]

$$\mathbf{A}\mathbf{K} + \mathbf{K}\mathbf{A}^T = -\mathbf{B}\mathbf{B}^T, \tag{40}$$

To solve for $\mathbf{K}$, we rewrite $\mathbf{K}$ as

$$\mathbf{K} = \begin{bmatrix} \mathbf{K}_1 & \mathbf{K}_2^T \\ \mathbf{K}_2 & K_{N+1} \end{bmatrix}. \tag{41}$$

where $\mathbf{K}_1$ is a symmetric square matrix $(N \times N)$. Since each particle x_i has the same covariance with y, we can express $\mathbf{K}_2$ as

$$\mathbf{K}_2 = k_2 \mathbf{w}, \tag{42}$$

where k_2 is a constant to be determined and $\mathbf{w}$ is defined in Eq.(26). Then, from

$$\mathbf{AK} + \mathbf{KA}^T = -\mathbf{BB}^T = -2 \begin{bmatrix} \mathbf{I}_N & \\ & 0 \end{bmatrix}, \tag{43}$$

we obtain

$$\begin{aligned} -2\mathbf{K}_1 + 2\alpha k_2 \mathbf{J}_N &= -2\mathbf{I}_N, & (44) \\ \frac{\Omega}{N} k_2 \mathbf{w}\mathbf{w}^T - 2K_{N+1}\Omega + \frac{\Omega}{N} k_2 \mathbf{w}\mathbf{w}^T &= 0, & (45) \\ -k_2 \mathbf{w}^T + \alpha \mathbf{w}^T K_{N+1} + \frac{\Omega}{N} \mathbf{K}_1 \mathbf{w}^T - \Omega k_2 \mathbf{w}^T &= 0, & (46) \end{aligned}$$

where

$$\begin{aligned} \mathbf{J}_N &= \mathbf{w}^T \mathbf{w}, \\ \mathbf{w}\mathbf{w}^T &= N. \end{aligned} \tag{47}$$

It is simple to solve the above equations making the use of Sherman-Morrison-Woodbury formula [4],

$$\begin{aligned} \mathbf{K}_1 &= \mathbf{I}_N + \alpha k_2 \mathbf{J}_N, & (48) \\ k_2 &= K_{N+1} = \frac{\Omega}{N(1-\alpha)(\Omega+1)}. & (49) \end{aligned}$$

Thus,

$$\langle x_i^2 \rangle = 1 + \frac{\alpha\Omega}{N(1-\alpha)(\Omega+1)}, \tag{50}$$

and by the definition the bias of $\langle x_i^2 \rangle$ in the presence of time-averaging is

$$B_{tav} = \frac{\Omega}{\Omega+1} \frac{\alpha}{N(1-\alpha)}. \tag{51}$$

Apparently, the smaller Ω is (the more time-averaging), the smaller the bias is.

On the other hand, by approaching $\Omega \to \infty$ in Eq.(51), we can easily obtain the solution of Eq.(13). The bias error for that case becomes

$$B_0 = \frac{\alpha}{N(1-\alpha)}. \tag{52}$$

We then can define the ratio b_{tav} as

$$b_{tav} = \frac{B_{tav}}{B_0} = \frac{\Omega}{\Omega + 1}. \tag{53}$$

The behavior of b_{tav} against Ω is shown in Fig.3. The following observations are made:

1. Each particle does not evolve independently, instead there is correlation among the particles although the correlation becomes weaker as N increases.

$$\langle x_i x_j \rangle = \frac{\Omega}{\Omega + 1} \frac{1}{N(1-\alpha)}, \qquad \text{for} \quad i \neq j. \tag{54}$$

   This means the particles do not constitute a set of independent samples. Note that the particles are correlated with y as well,

$$\langle x_i y \rangle = \frac{\Omega}{\Omega + 1} \frac{1}{N(1-\alpha)}, \qquad \text{for} \quad i = 1, \ldots, N. \tag{55}$$

2. The bias scales as $1/N$ in both cases, which has also been found in [12];

3. The time-averaging technique reduces bias by a factor of b_{tav};

4. The smaller Ω is, the smaller the bias is in the case with time-averaging (Recall that a longer time scale is introduced as a penalty);

5. For both cases, $\alpha \to 1$ leads to infinite bias. The system is unstable and does not have a stationary state.

3.3 Numerical Errors of A General System

It is then realized that a new estimate u of $\langle x \rangle$ can be defined by combining linearly $\{x\}$ and y

$$u = (1 - \beta) y + \beta \{x\}, \tag{56}$$

where β is a specified constant. Note that we will have $\langle u \rangle = \langle x \rangle$. For $\beta = 0$, we obtain the system of Eq.(15) and Eq.(16) while the system of Eq.(3) corresponds to $\beta = 1$. An arbitrary β forms the following system which can be solved as well

$$dx_i = -(x_i - \alpha u)dt + \sqrt{2} dW_i, \tag{57}$$

$$dy = -\Omega (y - \{x\}) dt. \tag{58}$$

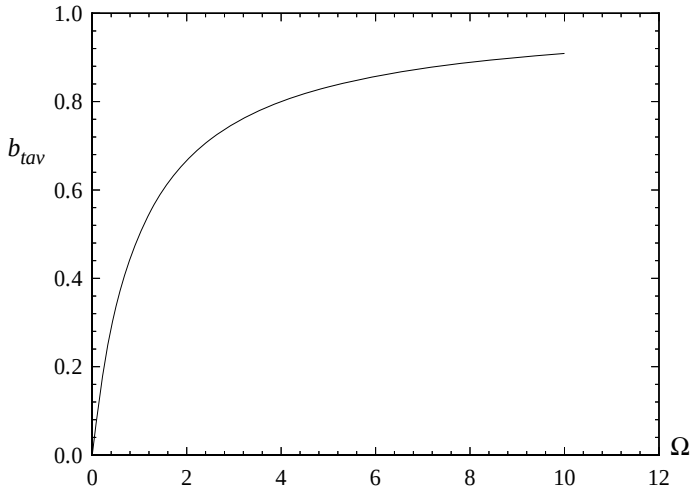

Figure 3: The behavior of b_{tav} against Ω

For the vector form of Eq.(22), we have

$$\mathbf{A} = \left[\begin{array}{cc} -\mathbf{I} + \frac{\alpha\beta}{N}\mathbf{J} & \alpha(1-\beta)\mathbf{w}^T \\ \frac{\Omega}{N}\mathbf{w} & -\Omega \end{array} \right]_{(N+1)^2}, \tag{59}$$

$$\mathbf{B} = \sqrt{2}\left[\begin{array}{cc} \mathbf{I} & 0 \\ 0 & 0 \end{array} \right]_{(N+1)^2}. \tag{60}$$

As the forgoing analysis, the variance matrix $\mathbf{K}$ can be written as

$$\mathbf{K} = \left[\begin{array}{cc} \mathbf{K}_1 & \mathbf{K}_2^T \\ \mathbf{K}_2 & K_{N+1} \end{array} \right], \tag{61}$$

and we have

$$-\mathbf{K}_1 + \frac{\alpha\beta}{N}\mathbf{K}\mathbf{J} + \alpha(1-\beta)\mathbf{w}^T\mathbf{w}k_2 = -\mathbf{I}_N, \tag{62}$$

$$\frac{\Omega}{N}\mathbf{w}\mathbf{w}^T k_2 - \Omega K_{N+1} = 0, \tag{63}$$

$$\frac{\Omega}{N}\mathbf{w}\mathbf{K}_1 - \Omega\mathbf{w}k_2 - \mathbf{w}k_2 + \frac{\alpha\beta}{N}\mathbf{w}k_2\mathbf{J} + \alpha(1-\beta)K_{N+1}\mathbf{w} = 0. \tag{64}$$

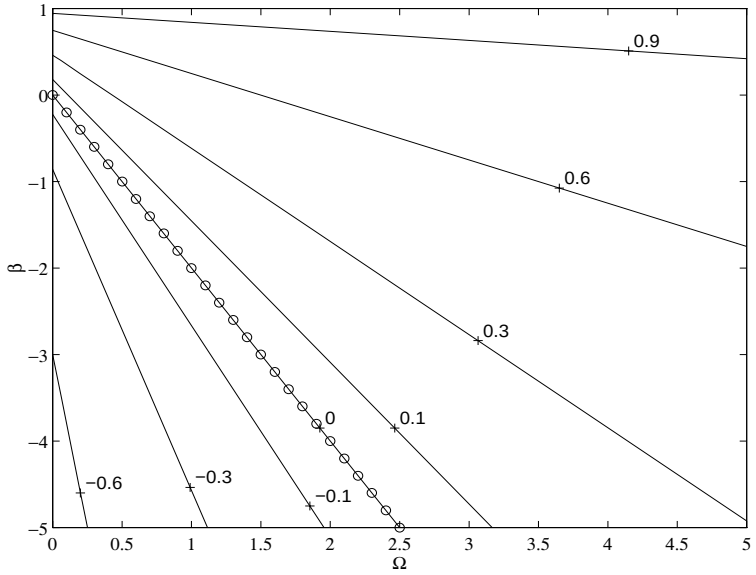

Figure 4: The contour plot of b_{gen} against β and Ω for $\alpha = 0.5$. $\circ$ corresponds to the line: $\beta = \Omega/(1-\alpha)$ along which the bias vanishes.

The solutions to these equations are

$$k_2 = K_{N+1} = \frac{1}{(1-\alpha)(\Omega+1-\alpha\beta)}\frac{\Omega}{N} \tag{65}$$

$$\mathbf{K}_1 = \mathbf{I}_N + \left[\frac{\alpha(1-\beta)}{(1-\alpha\beta)(1-\alpha)(\Omega+1-\alpha\beta)}\frac{\Omega}{N} + \frac{\alpha\beta}{N(1-\alpha\beta)}\right]\mathbf{J}_N. \tag{66}$$

The bias of $\langle x_i^2 \rangle$ for this general case is

$$B_{gen} = \frac{\alpha}{N(1-\alpha)}\frac{\alpha(1-\beta)\Omega}{(1-\alpha\beta)(\Omega+1-\alpha\beta)} + \frac{\beta(1-\alpha)}{N(1-\alpha\beta)}. \tag{67}$$

The ratio b_{gen} of B_{gen} to B_0 is calculated as

$$b_{gen} = \frac{B_{gen}}{B_0} = \left[\frac{(1-\beta)\Omega}{(1-\alpha\beta)(\Omega+1-\alpha\beta)} + \frac{\beta(1-\alpha)}{1-\alpha\beta}\right]. \tag{68}$$

Unlike b_{tav}, b_{gen} also depends on the value of α and β. As an example, Fig.(4) shows the behavior of b_{gen} as a function of β and Ω for $\alpha = 0.5$.

From Eq.(67) or Eq.(68), it is easy to find that if

$$\Omega = (\alpha-1)\beta \quad \text{or} \quad \beta = \frac{\Omega}{\alpha-1}, \tag{69}$$

then

$$B_{gen} = 0, \tag{70}$$

for $1-\alpha\beta \neq 0$ and $\alpha \neq 1$. In Fig.(4), the symbol represents the line of Eq.(69). Surprisingly, the bias vanishes in this case. It is also noticed that

$$\langle x_i x_j \rangle = \delta_{ij}, \tag{71}$$

$$\langle x_i u \rangle = 0. \tag{72}$$

That is, the particle properties turns out to be independent mutually and independent of the estimate of the mean. It is not difficult to verify from the particle equation that if an estimator for $\langle x \rangle$ in the particle equation satisfies the above conditions, the bias of the variance of x_i will vanish as well. Therefore, we can draw the conclusion that the numerical solutions of the particle Langevin equations have zero bias if and only if the particle properties are mutually independent, and independent of the estimate of the mean.

4 Conclusion

The numerical implementation of PDF methods for turbulent reactive flows leads to a system of stochastic differential equations consisting of a number of Langevin equations and an ordinary differential equation when the time-averaging technique is adopted. An analysis is carried on this stochastic differential system to explore the behavior of numerical errors in the PDF methods. It has been shown that the time-averaging technique with a large time scale can reduce the bias error. However, there is a disadvantage of time-averaging, that is the time-averaging introduces a longer time scale in the solution so as to take longer time to reach the stationary solution. A very interesting and important observation is that the particle samples are mostly not independent because the expectation in the Langevin equations has been replaced by an ensemble average of particles in the numerical calculation. This dependence results in the bias error. However, the time-averaging technique can be used to uncorrelate the particle samples so as to eliminate the bias if the estimate of the mean is approximated by a appropriate linear combination between the time averaged value and the ensemble average. The result of this study is applicable to a system of linear simplified

Langevin equations. The real model equations in the PDF methods are, however, highly non-linear. This analysis may not apply to that case, nevertheless it still provides a guideline for controlling the numerical errors in the PDF methods for turbulence modeling.

Acknowledgements

This work was suppported by the Air Force Office of Scientific Research, Grand F49620-94-1-0098.

REFERENCES

[1] L. Arnold. *Stochastic Differential Equations: Theory and Applications.* Krieger Publishing Company, 1974.

[2] E. Dedovic. An investigation of numerical error in the particle-mesh implementation of pdf methods for turbulent flows. Master's thesis, Cornell University, 1997.

[3] T. D. Dreeben and S.B. Pope. Nonparametric estimation of mean fields with application to particle methods for turbulent flows. Technical Report FDA 92-13, Cornell University, 1992.

[4] G.H. Golub and C.F. Van Loan. *Matrix Computations.* The Johns Hopkins University Press, 2nd edition, 1989.

[5] P.E. Kloeden and E. Platen. *Numerical Solution of Stochastic Differential Equations.* Springer-Verlag, 1992.

[6] S.B. Pope. Pdf methods for turbulent reactive flws. *Progress Energy and Combustion Science*, 11:119–192, 1985.

[7] S.B. Pope. Particle method for turbulent flows: Integration of stochastic differential equations. *J. Comput. Phys.*, 117:332–349, 1992.

[8] S.B. Pope. On the relationship between stochastic Lagrangian models of turbulence and second-moment closures. *Physics of Fluids*, 6(2):973–985, February 1994.

[9] S.B. Pope. *pdf2dv*. Cornell University, 1994.

[10] W.C. Welton and S.B. Pope. A PDF-based particle method for compressible turbulent flows. *AIAA Paper No. 95-0804*, 1995.

[11] J. Xu and S.B. Pope. Smoothing algorithms for pdf methods for turbulen flows. Technical Report To be issued as a FDA report, Cornell Universit, 1997.

[12] J. Xu and S.B. Pope. Sources of bias in particle-mesh methods for pdf models for turbulent flows. Technical Report FDA-9701, Cornell University, 1997.